Green Chemistry

PAPER

View Article Online
View Journal | View Issue

Check for updates

Cite this: *Green Chem.*, 2024, **26**, 3453

Functional deep eutectic solvent for lignocellulose valorization *via* lignin stabilization and cellulose functionalization†

Zhen Zhang, Pingli Lv, Hairui Ji, * Xingxiang Ji, Zhongjian Tian and Jiachuan Chen

This study shows a functional deep eutectic solvent (DES) employing choline chloride (ChCl) and glyoxylic acid (GA) for lignocellulose fractionation. This DES exhibited a higher pretreatment efficiency (92.15%) than that composed of ChCl and lactic acid (10.36%). Molecular dynamic (MD) simulations indicated that the ChCl : GA DES showed a higher total binding energy (ΔE) with lignin than the ChCl : LA DES, resulting in a higher dissolution of lignin. GA prevented lignin condensation during pretreatment. The stabilized lignin containing 69.39% β-O-4 linkages can be used for phenolic monomer production with a bio-oil yield of 59.60% and lignin-based sunscreen preparation with a SPF of 58.46. The cellulose residues with a mild pretreatment severity exhibited a high enzymatic saccharification yield of 91.99%. Meanwhile, an esterification reaction occurred between cellulose and GA during pretreatment. The inhibition of enzymatic hydrolysis and microbial growth enables the use of functional cellulose to produce antibacterial paper. Furthermore, 96.80% of the DES could be easily recycled and reused for biorefinery purposes.

Received 3rd December 2023,
Accepted 2nd February 2024

DOI: 10.1039/d3gc04749k

rsc.li/greenchem

Published on 02 February 2024. Downloaded on 5/23/2026 12:12:36 AM.

1. Introduction

Lignocellulosic biomass, a promising feedstock to replace petroleum resources for biofuel, chemical, and bioproduct production, has attracted much attention in recent years due to its sustainability, renewability, and carbon neutrality.[1,2] In the plant cell wall, hemicellulose and lignin encircle cellulose to form a rigid structure that is recalcitrant against degradation. The complex matrix hinders their further fractionation and value-added utilization for humans.[3,4] Thus, a pretreatment step is necessary to break down the recalcitrance towards efficient biomass conversion.[5,6]

So far, various pretreatment techniques have been developed to enhance the biomass fractionation, such as physical methods (*e.g.*, ball milling and microwave irradiation), chemical methods (*e.g.*, using ionic liquid and organic acid), biological methods (*e.g.*, using white-rot fungus), and physicochemical methods (*e.g.*, ammonia or alkali-steam explosion). Although these strategies promote enzymatic saccharification of glucan, their industrial applications face many challenges, such as cost and energy consumption.[7,8] DES, a typical eutectic mixture consisting of a hydrogen bond acceptor (HBA) and a hydrogen bond donor (HBD), has been identified as a promising media for biomass pretreatment due to its high lignin solubility, non-flammability, good bio-compatibility, and thermostability.[5,9,10] In particular, the ChCl-based DES exhibits an excellent ability to selectively dissolve lignin and hemicellulose from lignocellulosic biomass.[11,12] This is due to strong hydrogen bonds formed between hydroxyl groups (–OH) in the lignin-polysaccharide complex and the chloride ion (Cl^-) from ChCl.[1] Conversely, acidic protons in the HBD can promote the cleavage of ester bonds in lignin and hemicellulose, leading to their isolation from biomass.[4] Currently, widely used ChCl-based DESs include ChCl as a HBA and polyol and organic acids, such as glycerol, 1,4-butanediol (BDO), lactic acid (LA), oxalic acid (OA), acetic acid (AA), and *p*-toluenesulfonic acid (*p*-TsOH), as HBDs.[13–15] Although a high lignin dissolution (65%–90%) was obtained with the ChCl-based DES, an undesired condensation of lignin usually occurs by the formation of a C–C linkage during pretreatment, which dramatically affects the further upgrading of lignin.[16,17] For example, Wang *et al.* used a DES (ChCl and *p*-TsOH) for miscanthus pretreatment at 80 °C for 20 min, resulting in a low β-O-4 linkage content of only 30.90% in the obtained lignin.[18] Several researchers have developed diol-based DES systems containing glycol and ChCl to pretreat biomass and obtain functionalized lignin.[4,19,20] However, the delignification yield and lignin stabilization efficiency need to be improved. Recently, Bertella *et al.* used a cosolvent containing glyoxylic

Key Laboratory of Pulp and Paper Science & Technology of Ministry of Education, State Key Laboratory of Biobased Material and Green Papermaking, Faculty of Light Industry, Qilu University of Technology (Shandong Academy of Sciences), Jinan 250353, China. E-mail: jihairui@yeah.net

† Electronic supplementary information (ESI) available. See DOI: https://doi.org/10.1039/d3gc04749k

Published on 02 February 2024. Downloaded on 5/23/2026 12:12:36 AM.

acid (GA), dioxane, and HCl to extract lignin. GA addition efficiently prevented lignin condensation and simultaneously introduced a carboxyl group on the lignin backbone.[21] This gave us inspiration to use GA-containing carboxyl groups as HBDs to prepare a DES with ChCl as a HBA, achieving lignin extraction, stabilization, and functionalization.

In this study, a functional DES employing ChCl and GA was developed to pretreat lignocellulose for lignin stabilization and valorization toward multiple purposes. The effect of different pretreatment conditions on changes in main components during pretreatment was investigated. The lignin dissolution mechanism of the ChCl : GA DES was explored by a molecular dynamics (MD) simulation. After that, the value-added utilization of stabilized lignin was carried out, such as preparing phenolic monomers *via* hydrogenative depolymerization and producing lignin-based sunscreen. Furthermore, the enzymatic hydrolysis and antibacterial testing of obtained fibers after pretreatment were performed. By blending with softwood pulp, the obtained fibers were used for papermaking. In addition, the ChCl : GA DES was recycled for further reuse. Therefore, this green refining strategy provides a valuable reference for achieving a sustainable bioeconomy and highlights the potential for efficient pretreatment and conversion of lignocellulosic biomass using the ChCl : GA DES.

2. Experimental section

2.1 Materials

Boehmeria nivea stalks used in this study were kindly provided by Shandong Century Sunshine Paper Group Co., Ltd (Shandong, China). Chemical reagents of analytical grade, such as choline chloride (ChCl), lactic acid (LA), glyoxylic acid (GA), and dimethyl sulfoxide (DMSO), were purchased from Macklin Biochemical Technology Co., Ltd (Shanghai, China).

2.2 DES synthesis

ChCl and GA were mixed at different molar ratios (1 : 2, 1 : 3, 1 : 4 and 1 : 5) and subsequently heated for 30 min at 80 °C and 200 rpm to obtain a DES. Additionally, a DES composed of ChCl and LA with a molar ratio of 1 : 4 was used for comparison.

2.3 *Boehmeria nivea* stalk pretreatment

The *Boehmeria nivea* stalks were crushed into particles with a diameter of 0.45–0.9 mm using a grinder (FZ102, Tianjin Teste Instrument Co., Ltd, China). Subsequently, 3 g of those particles and 40 g of DES were added in a pressure vessel (P170003, Tchongqing Xinweier Glass Co., Ltd, China), and the pretreatment was carried out at different temperatures (110 °C, 120 °C, 130 °C, and 140 °C) and times (30 min, 60 min, 90 min, and 120 min), as illustrated in Table S1.† At the end of each reaction, the pressure vessel was cooled to room temperature before opening. After adding 50 mL of ethanol (EtOH) into the vessel and stirring for 30 min; solid and liquid phases were separated employing filter paper (15 cm, Shenzhen Xinkehua Experimental Instrument Co., Ltd, China). The solids were washed with ethanol (50 mL) and deionized water (DI) to a neutral pH, and subsequently subjected to ultrasonication for 10 s to form a pulp. EtOH was removed *via* rotary evaporation (XA-R-1010, Xi'an Yuhui Experimental Instrument Co., Ltd) at 40 °C and 100 rpm. The stabilized lignin was obtained from the liquid phase after precipitation with DI and filtration. The DES was recycled using rotary evaporation at 100 rpm for 60 °C for the next pretreatment of *Boehmeria nivea* stalks.

The component content in the pretreated solids was analyzed following the protocol described by the National Renewable Energy Laboratory (NREL).[22] This process involved adding 0.3 g of dry solids and 3 mL of 72% sulfuric acid to a pressure vessel and allowing it to soak for 2 h. After adding 84 mL of ultrapure water, the hydrolysis reaction was conducted at 121 °C for 1 h using a steam sterilizer. Monosaccharide concentrations in the liquid phase were measured using an HPLC system (Ultimate 3000, Thermo Scientific) equipped with a separating column (Aminex HPX-87H, Bio-Rad, CA, United States) and a refractive index detector (RID-20A, Shimadzu, Japan). The pretreatment efficiency was calculated using the following equation:[23]

$$E_{\text{pretreatment}}\,(\%) = \left(1 - \frac{m_{\text{lignin1}}/m_{\text{cellulose1}}}{m_{\text{lignin0}}/m_{\text{cellulose0}}}\right) \times 100\%, \quad (1)$$

where $E_{\text{pretreatment}}$ is the pretreatment efficiency (%); m_{lignin1} and $m_{\text{cellulose1}}$ are the weights of lignin and cellulose in the pretreated substrate, respectively (g); m_{lignin0} and $m_{\text{cellulose0}}$ are the weights of lignin and cellulose in the raw *Boehmeria nivea* stalks, respectively (g).

2.4 MD simulation of the lignin dissolution mechanism

MD simulations were performed using GROMACS 2018.4 software.[24–26] Veratrylglycerol-β-guaiacyl ether (VG) was used as a model compound of lignin for computer simulation.[27–29] The simulation system of the pure DES contained 510 Lac/Gac and 2040 choline chloride molecules. Before program running, the steepest descent method was used to minimize the simulation system. The simulation was equilibrated for 5 ns in the normal volume and temperature (NVT) ensemble and 40 ns in the normal pressure and temperature (NPT) ensemble (P = 1 bar). An additional 5 ns NPT ensemble simulation was carried out to collect representative snapshots. After adding a VG molecule into the DES simulation system, the DES-VG system simulation was run under same conditions as described above.

2.5 Cellulose residue characterization and utilization

The crystallinity index (CrI) of the cellulose residue was analyzed on an X-ray diffractometer (Ultima IV, Japan) with a diffraction angle range from 5° to 40° and a scanning speed of 2° min^{-1}. CrI was calculated using the following equation:

$$\text{CrI}(\%) = \frac{I_{002} - I_{\text{Amorph}}}{I_{002}} \times 100\%, \quad (2)$$

 This journal is © The Royal Society of Chemistry 2024

Published on 02 February 2024. Downloaded on 5/23/2026 12:12:36 AM.

where I_{002} and I_{Amorph} stand for the diffraction intensities at approximately $2\theta = 22°$ and 18°, respectively.

Fiber quality analysis (FQA), including fiber length and width, was performed on a L&W Fiber tester (ABB AB/Lorentzen & Wettre, Sweden) according to the TAPPI T-pm-91 standard.

Handsheets were prepared by blending softwood pulp and *Boehmeria nivea* pulp of various amounts (0%, 5%, 10%, 15%, and 20%, wt%) at a basis weight of 100 g m^{-2} in accordance with the SCAN-C 26:76 standard. The ring crush strength of the prepared handsheets was measured on a ring compressive strength tester (17–60, Testing Machines Inc., America) based on the TAPPI T822 om-11 standard, the tear strength was tested on a tearing tester (009, ABB AB/Lorentzen & Wettre, Sweden) according to the TAPPI T414 om-88 standard, and the tensile strength was tested using an Auto Tensile Tester (066, ABB AB/Lorentzen & Wettre, Sweden) in accordance with the TAPPI T494 om-81 standard. The morphology was scanned using an SEM system (TM4000 Plus, Japan Hitachi Nake high-tech enterprise).

The enzymatic hydrolysis of the fibers was conducted on a shaking bed incubator (THZ-100, Shanghai Bluepard Instruments Co., Ltd, China) at a temperature of 50° C and a speed of 180 rpm. Specifically, dry pretreated substrate (1 g) and cellulase (Cellic® CTec 2, Novozymes, China) with a cellulase loading of 15 FPU g^{-1} glucan were added into a sodium citrate buffer of 50 mL (pH 4.8). At different time intervals (3 h, 6 h, 12 h, 20 h, and 30 h), 400 μL of the supernatant was taken out and centrifuged at 8000 rpm for 5 min. The glucose content was measured *via* a biosensor analyzer (SBA-40E, Biological Institute of Shandong Academy Sciences, China). The yield of enzymatic hydrolysis was calculated using the following equation:

$$Y_{EH}(\%) = \frac{m_{glucose}}{m_{solids} \times \frac{C_{glucan}}{0.9}} \times 100\%, \quad (3)$$

where $m_{glucose}$ and m_{solids} stand for the weights of produced glucose in the enzymatic hydrolysate and used pretreated solid, respectively (g); C_{glucan} is the glucan content in the pretreated solid; 0.9 is a conversion coefficient from glucan to glucose.

To assess the antimicrobial capabilities of the prepared antibacterial paper using pretreated fibers, 100 μL of *Staphylococcus aureus* cultured in 50 mL of liquid medium was diluted with sterile water and poured onto a plate with solid medium containing 2% (w/v) agar. The plate containing antibacterial paper and *Staphylococcus aureus* was incubated at 37 °C for 24 h.

The ^{13}C NMR measurement of cellulose was carried out using a Bruker Avance NEO spectrometer (400WB, Bruker, Germany) at a spinning speed of 10 kHz (4.2 μs 90° pulses), a cross-polarization pulse of 2 ms, and a recycling delay of 3 s.

2.6 Lignin characterization and utilization

To explore the chemical structure characteristics of lignin samples, 2D-HSQC NMR measurement was carried out on an Avance NEO 600M spectrometer (Bruker, Germany). Before testing, 40 mg of lignin was dissolved in 0.5 mL of DMSO-*d*6 solution.[17]

The lignin depolymerization was carried out in a high-pressure reactor containing 0.15 g of lignin and 20 mL of methanol at 230 °C for 15 h with a Ru/C catalysis loading of 0.1 g. It is worth noting that the initial hydrogen pressure and the working hydrogen pressure were 1 MPa and 8 MPa, respectively. After cooling the reactor to 25 °C, the liquid phase containing depolymerization products was separated from the reacted mixture through filtration. Then, *n*-hexane was added to extract the depolymerization products. The resulting liquid phase was analyzed by a GC-MS system (QP2020, Shimadzu) with a HP-5 column. The *n*-hexane was removed using rotary evaporation (XA-R-1010, Xi'an Yuhui Experimental Instrument Co., Ltd). The yield of bio-oil was calculated based on the following equation:

$$Y_{bio\text{-}oil}(\%) = \frac{m_{bio\text{-}oil}}{m_{lignin}} \times 100\%, \quad (4)$$

where $m_{bio\text{-}oil}$ and m_{lignin} are the weights of bio-oil and used lignin, respectively (g).

The UV absorbance of the lignin sample was measured on a UV-vis spectrophotometer (Shimadzu, Japan) with a wavelength range from 290 nm to 400 nm. DMSO-lignin solution was added in a dialysis bag (31 mm, Beijing Tianan United Technology Co., Ltd, China) for 48 h to generate lignin nanoparticles (LNPs). The particle size and morphology of the LNPs were further analyzed using a zeta potential tester (ZEN3690, Malvern Instruments Ltd, UK) and an atomic force microscope (AFM) (Multimode8, Bruker, Germany), respectively.

After freeze-drying, LNPs were added to commercial sunscreen to prepare lignin-based sunscreens. Different amounts (1%, 2%, 3%, and 4%, wt%) of LNPs and commercial sunscreen were blended and stirred in the dark for 24 h. Subsequently, the UV transmittance (T) of the prepared sunscreen was tested within a wavelength region of 290 nm–400 nm and a slit width of 5 nm. Prior to testing, the prepared sunscreen was coated on a 3 M medical tape on a clean quartz glass slide with a coating weight of 2 mg cm^{-2}. The sun protection factor (SPF) was calculated according to the following equation based on previous literature:[6,30]

$$SPF = \sum_{290}^{400} E_\lambda S_\lambda / \sum_{290}^{400} E_\lambda S_\lambda T_\lambda \quad (5)$$

where E_λ, S_λ and T_λ stand for erythemal spectral effectiveness, solar spectral irradiance, and spectral transmittance, respectively.

Published on 02 February 2024. Downloaded on 5/23/2026 12:12:36 AM.

3. Results and discussion

3.1 *Boehmeria nivea* stalk pretreatment

The effect of different pretreatment parameters, such as pretreatment temperature (T), molar ratio (M), and pretreatment time (t), on the changes in the main components of the pretreated solid during pretreatment was investigated. Fig. 1a shows the effect of temperature on the cell wall compositions of the pretreated substrates. Accordingly, the content of the main components can be seen in Table S2.† Hemicellulose of 47.68% and lignin of 19.46% were removed from raw materials at 110 °C. Increasing the temperature from 110 °C to 140 °C caused obvious delignification and hemicellulose removal. Only 4.13% of hemicellulose and 4.32% of lignin were found in the pretreated solid at 130 °C compared with initial contents in the raw material (hemicellulose of 22.46% and lignin

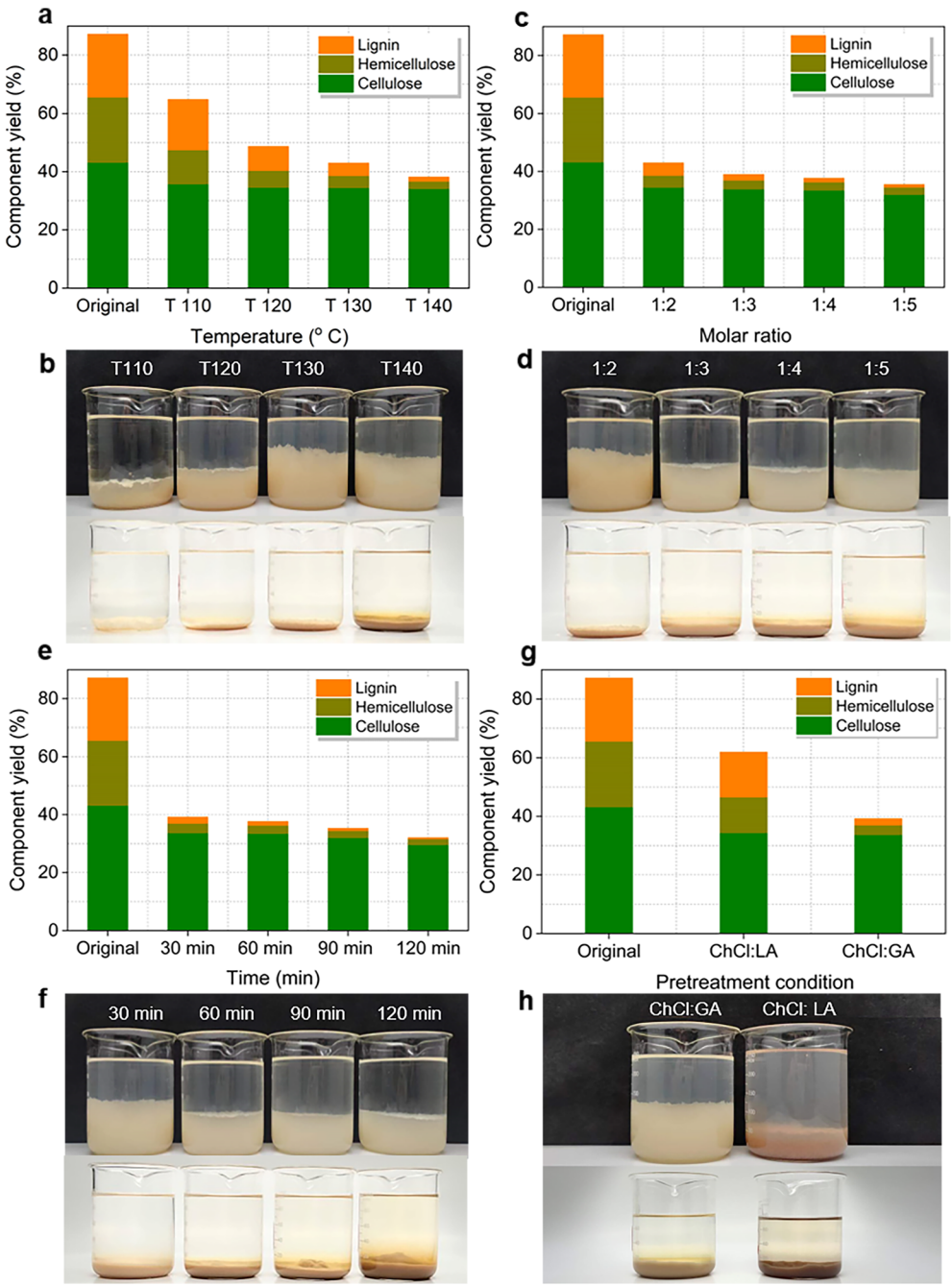

Fig. 1 The changes in the three main components of the pretreated solids at different pretreatment temperatures (a), molar ratios (c), and pretreatment times (e); the morphology of the pulp (top) and stabilized lignin (bottom) at different pretreatment temperatures (b), molar ratios (d), and pretreatment times (f); a comparison of the changes in the three main components (g) and morphology of the pulp (top) and stabilized lignin (bottom) (h) between ChCl : GA and ChCl : LA with same pretreatment conditions.

This journal is © The Royal Society of Chemistry 2024

Published on 02 February 2024. Downloaded on 5/23/2026 12:12:36 AM.

of 21.53%). Under this pretreatment temperature, an obvious fiber dissociation occurred after 10 s of ultrasonic treatment (Fig. 1b). However, an increased pretreatment temperature caused a high energy consumption and serious cellulose degradation. Therefore, a relatively mild pretreatment temperature of 130 °C was determined with a high removal of lignin (79.93%) and hemicellulose (81.61%). After that, the effect of the molar ratio of ChCl : GA on the changes in the main components of the cellulose residues was further explored at 130 °C (Fig. 1c). As the molar ratio increased from 1 : 2 to 1 : 5, the retention rate of hemicellulose and lignin decreased from 4.13% and 4.32% to 2.54% and 0.96%, respectively (Table S2†). The viscosity of the DES presented in Table S3† further supported the above observation that an increase in the GA content in the DES led to a decrease in viscosity, resulting in improved flowability, which promoted the pretreatment efficiency.[31] The fibers were released from the pretreated matrix (Fig. 1d). It should be noted that the content of cellulose partially reduced from 34.50% to 31.97% (Table S2†) as the molar ratio increased. Furthermore, the presence of excessive GA in the DES solution further affected the saccharification yield in enzymatic hydrolysis. The pretreatment efficiency under molar ratios of 1 : 4 reached 92.15%. Therefore, an appropriate molar ratio of 1 : 4 with high-pretreatment efficiency (>90%) was chosen. According to the results in Fig. 1e and Table S2,† and the morphology of the stabilized lignin (Fig. 1f), the optimum pretreatment time was determined to be 30 min. Only 3.33% of hemicellulose and 2.15% of lignin remained in the cellulose residue. Although prolonging the pretreatment time resulted in an increase of the pretreatment efficiency, cellulose would be degraded accompanied by the destruction of the lignin structure. Higher temperature enhanced the removal of lignin and hemicellulose from the amorphous region. The CrI of the cellulose residue also increased (Fig. S1b†). Increasing the molar ratio and extending the pretreatment time showed a decrease of CrI. For example, an obvious CrI decrease from 75.45% to 72.40% was found as the pretreatment time which further prolonged from 30 min to 120 min. The main reason was that the swelling of the crystalline region of cellulose was promoted after DES penetration.[32] In addition, the CrI decreased from 74.65% (1 : 3) to 72.48% (1 : 5) because the acid hydrolysis of cellulose in the crystalline region occurred due to the presence of GA. Therefore, the optimal pretreatment conditions were determined as a pretreatment temperature of 130 °C, a molar ratio (ChCl : GA) of 1 : 4, and a pretreatment time of 30 min.

A pretreatment comparison was carried out between ChCl : GA and ChCl : LA with the same pretreatment conditions as for T130M1:4t30. Fig. 1g and h show the changes in the three main components and morphology of the pulp (top) and stabilized lignin (bottom). Only 28.66% of lignin and 45.73% of hemicellulose were removed from the *Boehmeria nivea* stalks for ChCl : LA. After pretreatment with ChCl : GA, the CrI of the cellulose residue increased from 65.96% to 75.45% as hemicellulose and lignin were dissolved out from the raw materials. Compared with the ChCl : GA DES pretreatment, the ChCl : LA DES pretreatment led to a lower CrI under same pretreatment conditions (Fig. S1a†). The pretreatment efficiency of the ChCl : GA DES reached 92.15%, which was 8.89 times higher than that of the ChCl : LA DES (10.36%) under same conditions of T130M1:4t30, demonstrating a strong ability for lignin and hemicellulose extraction. Moreover, the obtained lignin with ChCl : LA DES exhibited a darker brown color than that of ChCl : GA DES. Furthermore, the collected cellulose residue cannot be effectively dispersed in water to form a pulp after ultrasonic treatment (Fig. 1h).

3.2 MD simulation of the lignin dissolution mechanism

To understand the interactions between lignin and DES molecules, the lignin dissolution mechanism of the ChCl : GA DES, and the reason for differences in lignin removal between ChCl : GA and ChCl : LA DESs, MD simulations were performed using VG as a model compound of lignin. The densities of the two DESs were first calculated to ensure the accuracy of the parameters employed in the MD simulations.[13] The calculated densities of ChCl : GA and ChCl : LA DESs were 1.25 g cm^{-3} and 1.39 g cm^{-3}, as shown in Fig. S2,† respectively, which was consistent with the measured densities of 1.23 g cm^{-3} and 1.36 g cm^{-3} with a permitted error of below 2.00%. The force field parameters used in the simulation are very reliable. Fig. 2 shows the volumetric density map (isosurface) of cosolvent molecules around the VG molecule at different isovalues. Based on the results from Fig. 2a and the movie in the ESI,† the distance between ChCl : GA and VG is closer than that between ChCl : LA and VG. Subsequently, the local organization and bonding of the DES molecules in the immediate vicinity of VG were investigated by calculating radial distribution functions (RDFs) between the DES and VG molecules, or more precisely, by calculating the center of mass (the molecule) RDFs, as shown in Fig. 2b. For the simulation system of Lac/ChCl-VG, an obvious sharp peak was found at 5.36 Å with a strength value of 1.97 for the centroids of the ChCl : LA and VG benzene ring, while a strong peak with a strength value of 2.23 appearing at 4.50 Å for the centroids of the ChCl : GA and VG benzene ring in the simulation system of Gac/ChCl-VG. The two strong peaks approaching around 5.00 Å were attributed to the H–π interaction between the VG benzene ring and DES molecules, thus resulting in high strength of van der Waals interaction.[12] The results were consistent with those in Fig. 2a. Furthermore, interaction energies (ΔE), mainly van der Waals (LJ-SR) and electrostatic (Coul-SR) interaction energies, between the DES and VG molecules were calculated, as shown in Fig. 2c. The electrostatic interaction energies of ChCl/LA-VG and ChCl/GA-VG were calculated to be 161.19 kJ mol^{-1} and 158.35 kJ mol^{-1}, respectively. No significant difference in electrostatic interaction energy was found between the two simulation systems. The electrostatic interactions were cumulated according to the cutoff method with a distance of 3.0 nm. The calculated van der Waals interaction energies of Lac/ChCl-VG and Gac/ChCl-VG were 215.63 kJ mol^{-1} and 234.55 kJ mol^{-1}, respectively, indicating that van der Waals interaction plays an important role in the interaction between the DES and VG mole-

Published on 02 February 2024. Downloaded on 5/23/2026 12:12:36 AM.

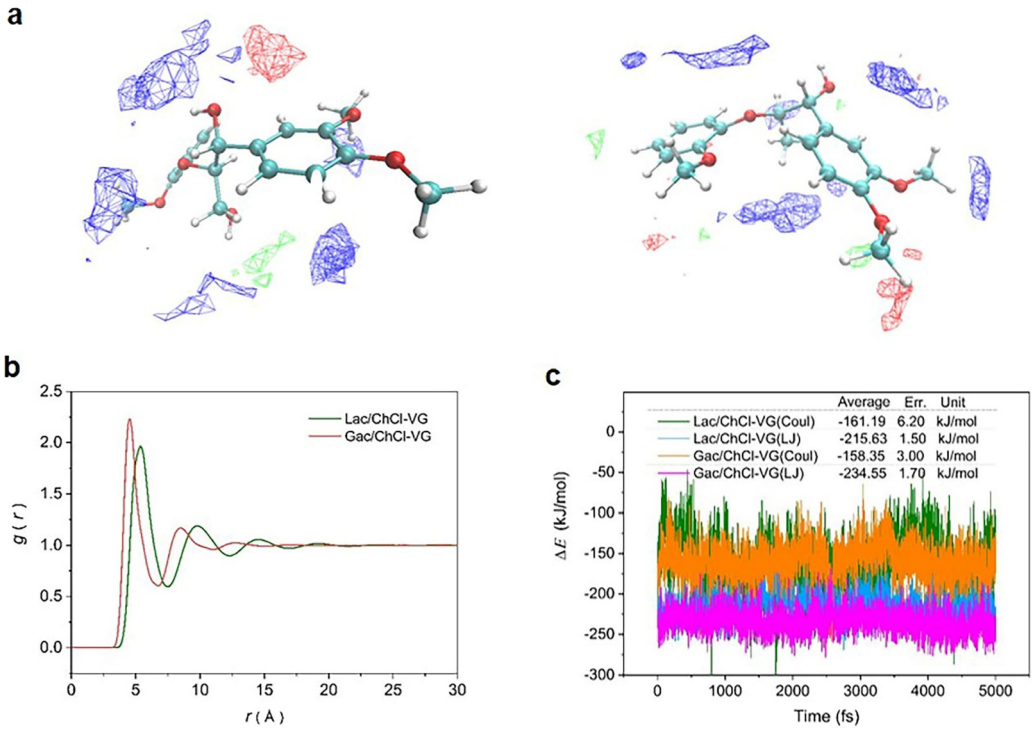

Fig. 2 (a) Volumetric spatial density maps (isosurfaces) of the time averaged distribution of the cosolvent and molecules (red, green and blue isosurfaces represent ChCl cations, ions, and acid molecules, respectively); the isovalues of the ChCl cation, ion, and Lac molecules for the complex of ChCl : LA and VG are 0.02, 0.004, and 0.02, respectively; the isovalues of the choline chloride cation, ion, and Gac molecules for the complex of ChCl : GA and VG are 0.02, 0.004, and 0.02, respectively. (b) The RDFs of the DES and VG molecules. (c) The calculated interaction energies between the DES and VG molecules, mainly van der Waals (LJ-SR) and electrostatic (Coul-SR) interaction energies.

cules. The ChCl : GA DES system with a high total ΔE of 392.90 kJ mol^{-1} caused a higher dissolution of lignin than the ChCl : LA DES system (376.82 kJ mol^{-1}), which explains why using the ChCl : GA DES lead to a higher lignin removal during pretreatment than using the ChCl : LA DES.

3.3 Characterization and utilization of cellulose

Fiber length and width were measured through FQA as presented in Table S4.† The fiber length and width decreased from 0.48 mm and 44.90 μm to 0.37 mm and 25.10 μm, respectively, with an increase in temperature from 110 °C to 140 °C. At 130 °C, almost all of the fibers had dissociated from the pretreated solid to form a pulp (Fig. 1b). The length and width were measured to be 0.35 mm and 25.30 μm, respectively. High temperature caused hydrolysis of the cellulose chain, resulting in a short fiber length. This conclusion is further substantiated by the SEM image presented in Fig. S3.† Thus, the fibers from the pretreatment conditions of T130M1:4t30 were used for papermaking by blending them with commercial softwood pulp.

The saccharification yield of the cellulose residues after various pretreatment conditions (Table S5†) was investigated, as shown in Fig. 3a. The ChCl : GA DES pretreatment resulted in a higher cellulose digestibility rate of 70.61% than that using the ChCl : LA DES pretreatment (60.91%) under same conditions (130 °C). This was due to the removal of more hemicellulose and lignin during the pretreatment process, which led to an increased surface area for enzyme adsorption.[16] The SEM images of the pretreated substrates also revealed a loose structure (Fig. 3c). After 10 s of ultrasonic treatment, the free fibers were released from the pretreated matrix (Fig. 3c) to form a pulp (Fig. 1b). Interestingly, the highest saccharification yield of 91.99% was found after 30 h of enzymatic hydrolysis for the cellulose residue with a pretreatment temperature of 110 °C. The increased pretreatment temperature caused a decrease of the enzymatic efficiency (Fig. 3a). The main reason for this was the chemical modification of cellulose by the esterification reaction between the carboxyl groups in GA and hydroxyl groups in cellulose during pretreatment (Fig. 3d). The aldehyde groups on the surface of cellulose caused a possible inhibition or deactivation effect on the individual cellobiohydrolase (CBH) and β-glucosidase (BG) activities. In particular, enzyme deactivation is usually indicated by a time-dependent loss of enzyme activity. Aldehyde groups could interact with different functional groups on the enzyme/protein surface through covalent and/or exceptionally strong noncovalent bonds, which sometimes remain even after complete protein breakdown.[33,34] This finding was demonstrated in the FTIR spectrum of the pretreated substrates (Fig. 3b). A new signal was found at 1202 cm^{-1} originating from the stretching vibration of the CO–O–C structure in the ester bond.[35] A clearer peak was observed in the substrate as

 This journal is © The Royal Society of Chemistry 2024

Published on 02 February 2024. Downloaded on 5/23/2026 12:12:36 AM.

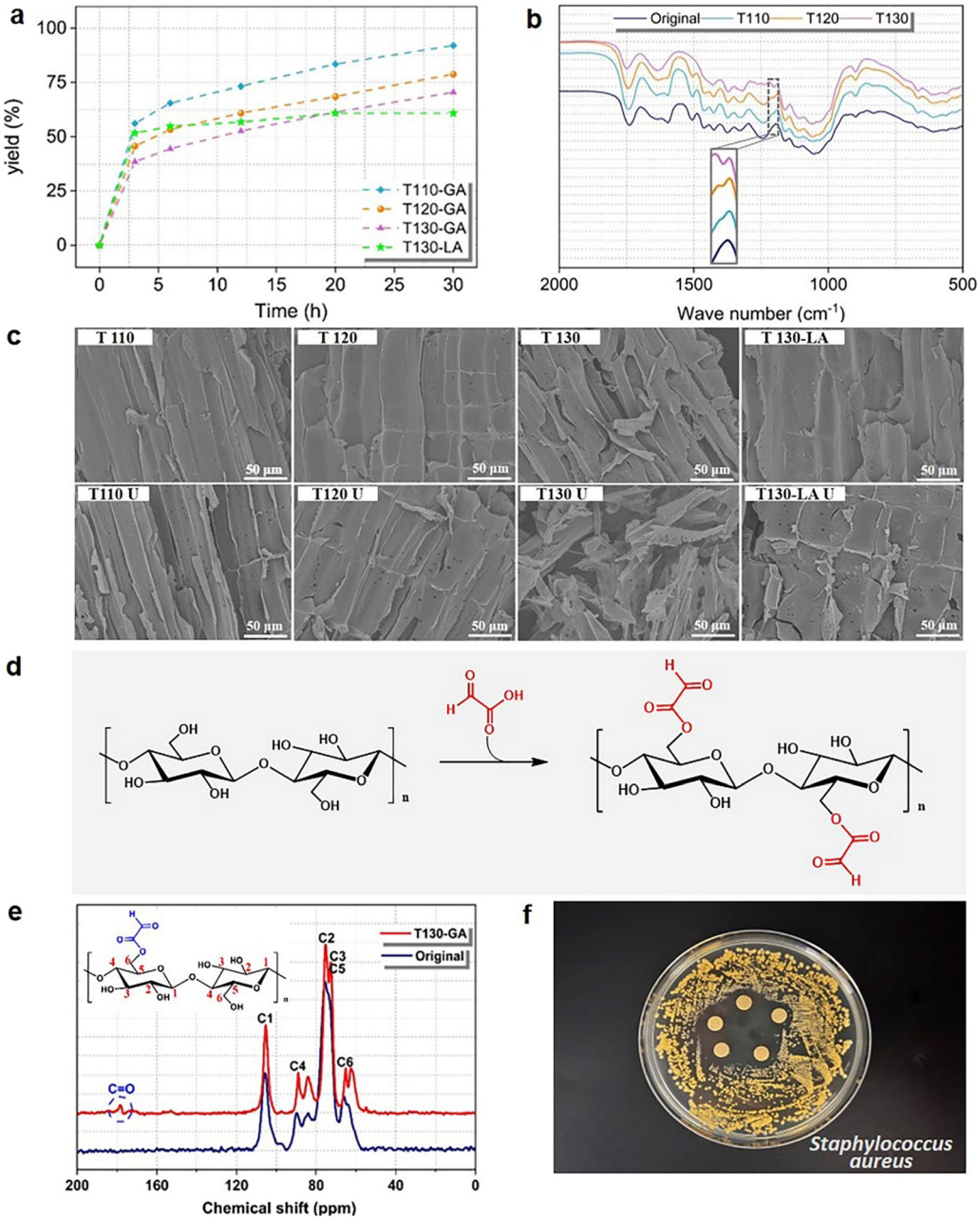

Fig. 3 (a) The saccharification yield of cellulose residues; (b) the FTIR spectrum of the pretreated substrates; (c) SEM images of the pretreated solids (*Tx* stands for pretreatment temperature and *U* stands for a 10 s ultrasonic treatment); (d) the esterification reaction between cellulose and GA during the pretreatment process; (e) the ^{13}C spectrum of the pretreated substrate; (f) a digital photo of antimicrobial measurement of the prepared paper using the fibers from the pretreatment conditions of T130M1:4t30.

the pretreatment temperature was raised. Furthermore, the solid-state ^{13}C NMR spectra of the pretreated substrates exhibited a typical carbonyl group peak at 178 ppm in Fig. 3e, further revealing that an esterification occurred between cellulose and GA during the pretreatment process.[36] In short, the ChCl : GA DES pretreatment resulted in not only a high yield (91.99%) of enzymatic saccharification when converting the cellulose residue to glucose but also cellulose functionalization by introducing aldehyde groups on the cellulose surface. The inhibition on enzymatic hydrolysis gave us inspiration to use the esterified cellulose to produce antibacterial paper. Fig. 3f demonstrates the good inhibitor effect of the prepared antibacterial paper towards the growth of *Staphylococcus aureus* within 24 h.

The physical properties, such as ring crush strength index, tear index, and tensile index, of the handsheets produced by mixing commercial softwood pulp with *Boehmeria nivea* pulp are shown in Fig. 4. Although the average length of the

Published on 02 February 2024. Downloaded on 5/23/2026 12:12:36 AM.

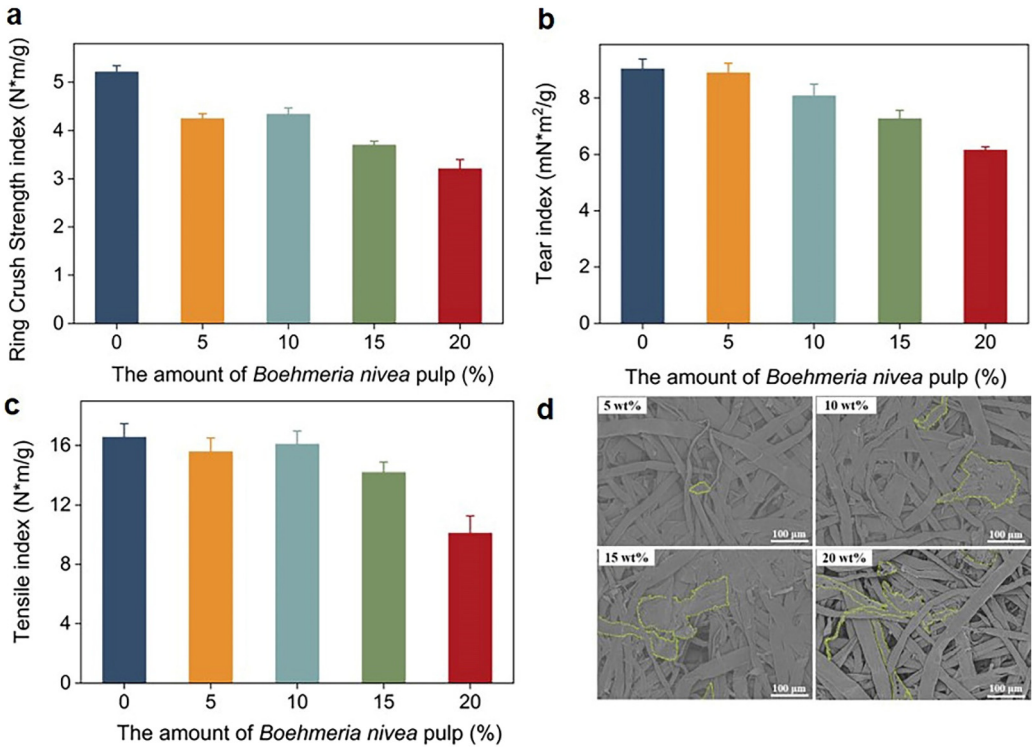

Fig. 4 The physical properties and SEM images of the prepared handsheets. (a) The ring crush strength index; (b) the tear index; (c) the tensile index; (d) the SEM images of the prepared handsheets with different amounts of *Boehmeria nivea* pulp.

Boehmeria nivea pulp is shorter than that of the commercial softwood pulp, some studies have shown that adding short fibers into the softwood pulp could improve the physical properties, particularly the ring crush strength index. This is because short fibers can fill up gaps between long softwood pulp fibers, leading to an increase in binding sites between the fibers. The enhancement of hydrogen bonding between hydroxyl groups on the fiber surface resulted in an improvement in the paper strength. In this study, although adding different amounts of *Boehmeria nivea* pulp into the softwood pulp did not significantly increase the mechanical strength of the handsheets, when the added amount of *Boehmeria nivea* pulp reached 10%, the mechanical strength was very close to that of the pure softwood pulp handsheets without *Boehmeria nivea* pulp addition. The ring crush strength index of 4.34 Nm g^{-1} (Fig. 4a), tear index of 8.07 mN m^2 g^{-1} (Fig. 4b), and tensile index of 16.09 Nm g^{-1} (Fig. 4c) of the prepared handsheets were 83.30%, 89.37%, and 97.16% of those of the pure softwood pulp handsheets, respectively. The probable reason was that the *Boehmeria nivea* fibers acted as a filler in the softwood fiber frame, and the gaps between the fibers were filled, not only increasing the binding sites but also improving the interactions of intermolecular hydrogen bonds (Fig. 4d).[6] However, further raising the amount of produced pulp significantly reduces the mechanical strength of the handsheets due to the decrease of softwood fibers. Thus, using *Boehmeria nivea* pulp to replace commercial softwood pulp at an optimum amount of 10% can reduce the cost of papermaking with a bit of bacterial inhibition function while providing a strategy for the utilization of agricultural waste, *Boehmeria nivea* stalks.

3.4 Lignin characterization and utilization

The ChCl : GA DES not only showed a higher lignin removal than ChCl : LA but also obtained a lighter colored lignin. Traditional lignin fractionation usually involves reactions of condensation and repolymerization to produce a highly stable C–C linkage. Aldehyde-assisted fractionation with GA can prevent lignin fractionation to form condensed lignin, as shown in Fig. 5a.[37] The structural characteristics of the extracted lignin with ChCl : GA DES, labeled as GSL, were analyzed *via* 2D HSQC NMR as demonstrated in Fig. 5g and h. Milled wood lignin that was labeled as MWL (Fig. 5c and d) and the extracted lignin with ChCl : LA DES that was labeled as LAL (Fig. 5e and f) were used for comparison.

As shown in Fig. 5, the 2D HSQC NMR spectrum was divided into a side chain region and a benzene ring region at δ_C/δ_H 52.0–100.0/2.70–5.30 ppm and δ_C/δ_H 100.0–136.0/6.30–8.00 ppm, respectively. The main cross-peaks are listed in Table S6† based on a previous publication.[38]

In the side chain region, a clear cross-signal of methoxy groups ($-OCH_3$) was observed at δ_C/δ_H 56.1/3.76 ppm. The typical interunit linkages, such as β-O-4 structure (A and A′ unit), phenyl-coumaran structure (β-5, B unit), and resinol (β-β, C unit), were also determined. Specifically, the cross-peaks for β-O-4 were displayed at δ_C/δ_H 72.1/4.88 ppm (Aα), δ_C/δ_H 84.1/

 This journal is © The Royal Society of Chemistry 2024

Published on 02 February 2024. Downloaded on 5/23/2026 12:12:36 AM.

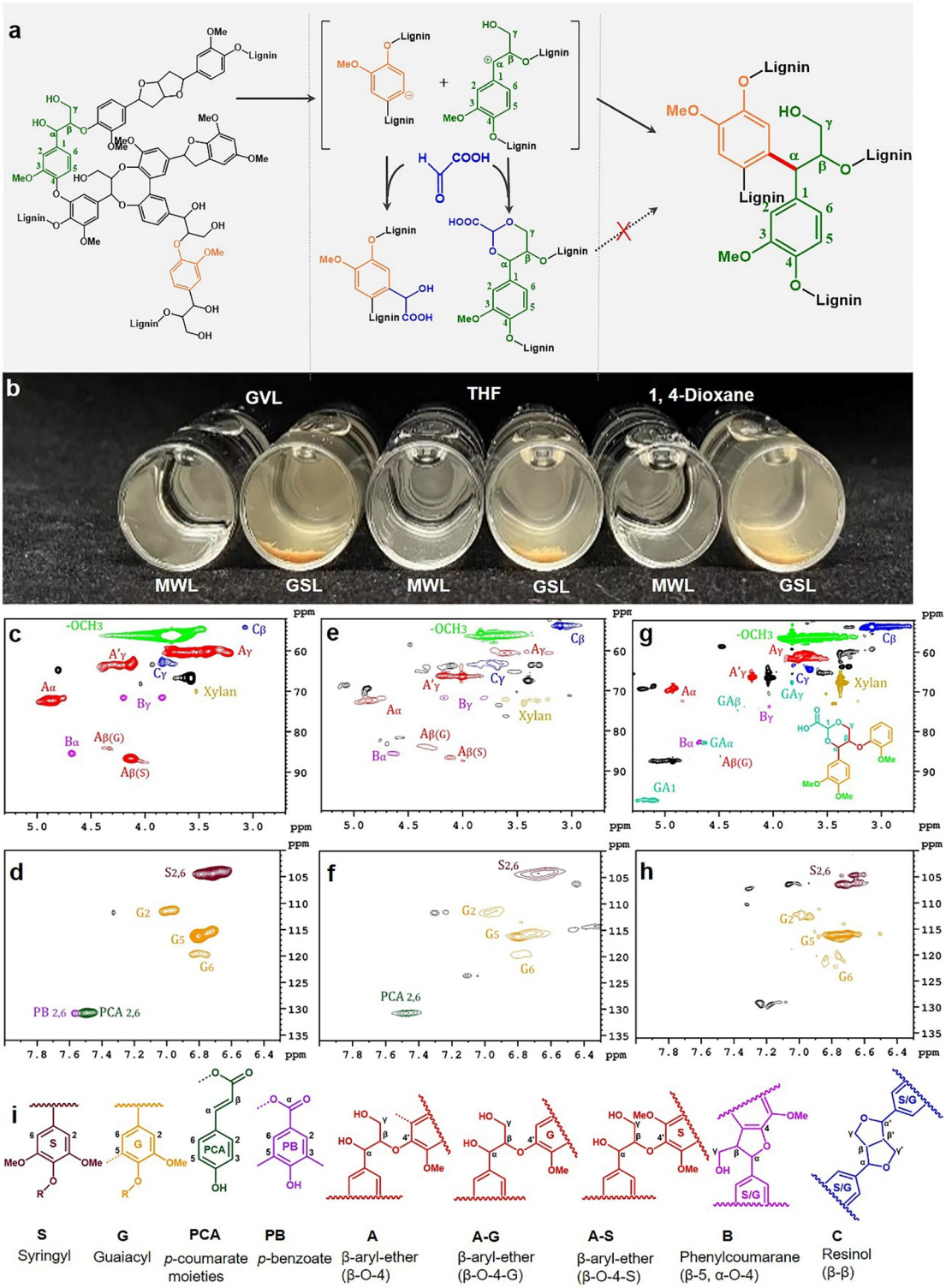

Fig. 5 Lignin stabilization mechanism and the HSQC spectra of different lignin samples. (a) Stabilization mechanism during lignin extraction; (b) a digital photo of MWL and GSL in different solvents (GVL, THF, and 1,4-dioxane); (c), (e) and (g) the side chain region of MWL, LAL and GSL, respectively; (d), (f) and (h) the benzene ring region of MWL, LAL and GSL, respectively; (i) the main chemical structure in *Boehmeria nivea* lignin.

4.35 ppm (Aβ(G)), δ_C/δ_H 87.0/4.13 ppm (Aβ(S)), δ_C/δ_H 60.0/3.72 ppm (Aγ), and δ_C/δ_H 63.5/4.25 ppm (A′γ). The phenyl-coumaran structures were found at δ_C/δ_H 85.2/4.69 ppm (Bα) and δ_C/δ_H 71.9/3.87–4.21 ppm (Bγ). The cross-signals at δ_C/δ_H 87.9/5.48 ppm (Cα), δ_C/δ_H 53.8/3.08 ppm (Cβ), and δ_C/δ_H 62.8/3.85 ppm (Cγ) were assigned to the resinol structure.[14] Unlike

Published on 02 February 2024. Downloaded on 5/23/2026 12:12:36 AM.

the spectra of MWL (Fig. 5c) and LAL (Fig. 5e), the cross-peak at δ_C/δ_H 97.0/5.06–5.27 ppm was attributed to the newly formed acetal structure (Fig. 5g).[39] Additionally, the α, β, and γ signals of stable lignin were observed at δ_C/δ_H 82.0/4.63 ppm, δ_C/δ_H 73.5/4.30–4.40 ppm, and δ_C/δ_H 67.0/3.82 ppm in Fig. 5g, respectively, which indicated that GA prevented further lignin condensation during the ChCl : GA DES pretreatment.[21] After stabilization and functionalization, the GSL exhibited a very poor solubility in GVL, THF, and 1,4-dioxane, as shown in Fig. 5b.

In the benzene ring region, the typical cross-signals of lignin were found, such as syringyl (S) and guaiacyl (G) units at δ_C/δ_H 104.2/6.72 ppm ($C_{2,6}$–$H_{2,6}$, S unit), δ_C/δ_H 111.1/6.95 ppm (C_2–H_2, G unit), δ_C/δ_H 116.1/6.81 ppm (C_5–H_5, G unit), and δ_C/δ_H 119.5/6.82 ppm (C_6–H_6, G unit),[40] respectively. Additionally, the peaks at δ_C/δ_H 131.1/7.57 ppm and δ_C/δ_H 130.8/7.50 ppm originated from *p*-benzoate units ($C_{2,6}$–$H_{2,6}$) and *p*-coumarate moieties ($C_{2,6}$–$H_{2,6}$, PCA unit). Table S7† illustrates the content of main inter-unit linkages (β-O-4, β-5, and β–β) and S/G ratio in the lignin samples. The GSL sample exhibited a high content of β-O-4 linkages (69.39%), which is very close to that of MWL (85.57%). The results indicated that the DES containing GA can effectively hinder the polymerization of lignin during lignin extraction.

The depolymerization of GSL was performed using Ru/C as a catalyst and methanol as a solvent at 230 °C for 15 h in hydrogen atmosphere. The original depolymerization analysis of the three lignin samples by gas chromatogram (MWL, LAL and GSL) is listed in Fig. S4.† As shown in Fig. 6, nine main aromatic monomers were found in the depolymerization products of MWL with a bio-oil yield of 81.10%. Six major lignin monomers were identified in the products of GSL with a bio-oil yield of 59.60%. Without GA stabilization during pretreatment, the bio-oil yield of 58.95% was obtained in the products of LAL. The ChCl : LA DES pretreatment showed a monomer yield of only 48.20% and low lignin removal (28.66%). The ChCl : GA DES pretreatment led to not only a high lignin removal (90.01%) but also a high final monomer yield after hydrogenolysis of the extracted lignin (57.80%). The increased monomer yield can be attributed to the stabilization mechanism in Fig. 5a, which is consistent with previous publications with FA stabilization.[40] The β-O-4 structure was largely preserved *via* preventing the formation of stable C–C bond linkages during the ChCl : GA DES pretreatment process. Therefore, GSL has great potential in the preparation of biofuels with excellent combustion performance by further catalytic hydrogenation.[41,42]

The stabilized lignin showed a strong UV absorption ability and could be used as an anti-ultraviolet additive for lignin-based sunscreen preparation.[6] After introducing an amount of carboxyl groups, the UV absorption ability of GSL was improved (Fig. 5a). Thus, the possibility of using the obtained GSL for lignin-based sunscreen production was investigated. To improve the dispersibility and UV resistance in sunscreen, the GSL was prepared into lignin nanoparticles (LNPs). The size distributions of the produced LNPs from different pretreatment conditions are shown in Fig. S5.† The different LNPs exhibited a similar size distribution between 100 and 1000 nm, indicating that these LNPs had a larger specific surface area and could provide stronger UV shielding function. Furthermore, these uniform-size LNPs were dispersed in commercial emulsions to prepare lignin-based sunscreens (Fig. 7a).

The UV absorptions of the LNPs extracted at different temperatures were measured prior to preparing sunscreen as pre-

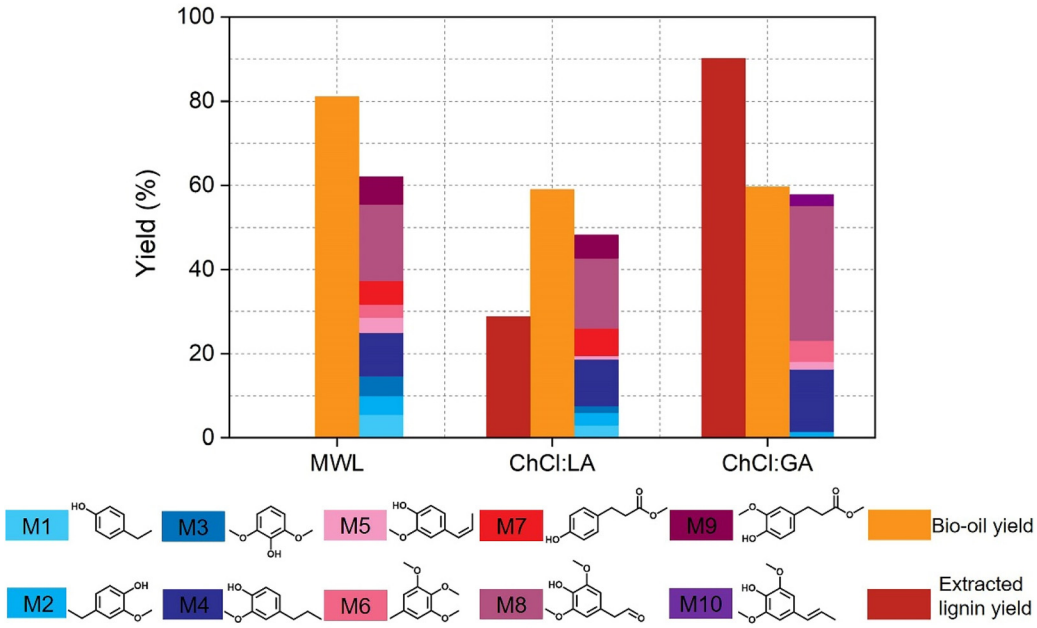

Fig. 6 The bio-oil and aromatic monomer yields of lignin (MWL, LAL, and GSL) after depolymerization.

 This journal is © The Royal Society of Chemistry 2024

Published on 02 February 2024. Downloaded on 5/23/2026 12:12:36 AM.

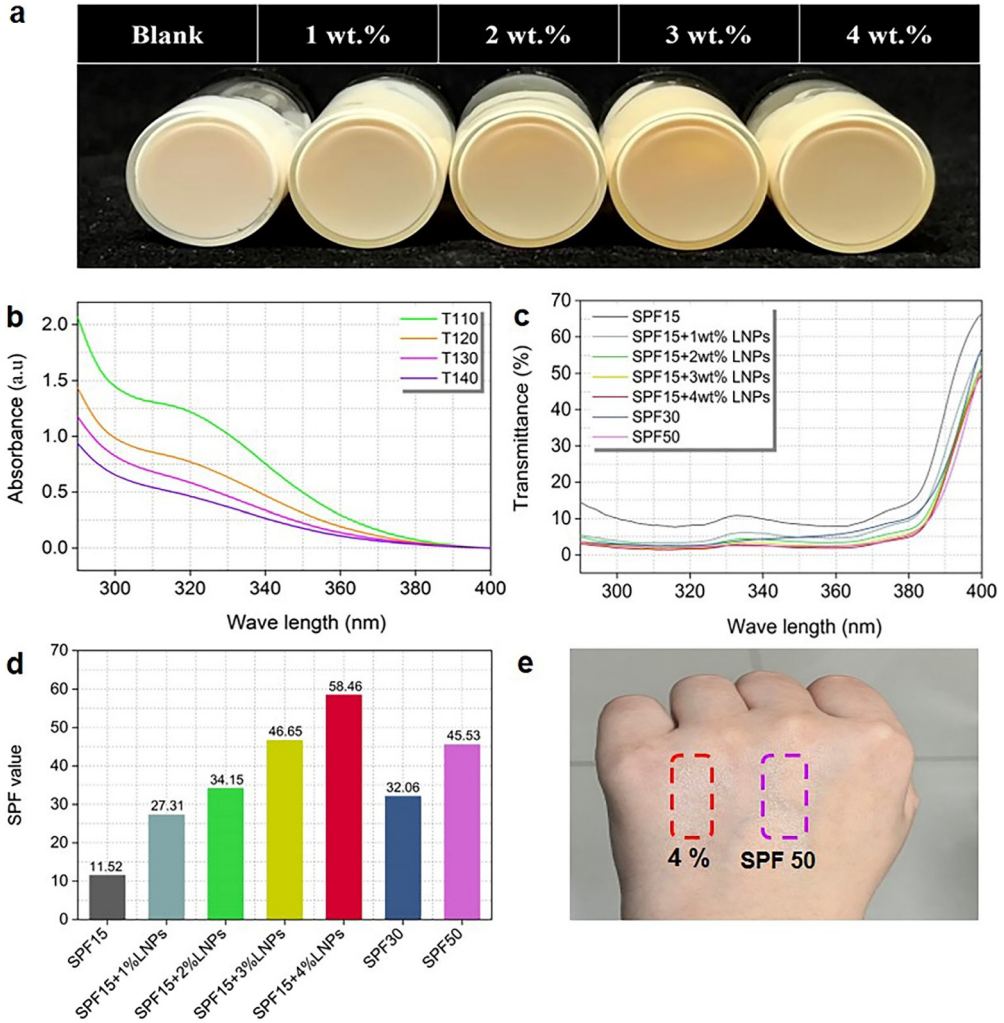

Fig. 7 (a) Digital photo of the prepared sunscreen by adding different amounts of LNPs; (b) UV absorbance curves of different LNPs; (c) UV transmittance curves of different sunscreens; (d) measured SPF value of the prepared sunscreen and commercial sunscreen; (e) contrast photo of the UV absorbance using the prepared sunscreen (4% LNPs addition) and commercial sunscreen (SPF 50) on the back of the hand.

sented in Fig. 7b. The UV absorption of the LNPs decreased with the temperature rising. The LNPs obtained at 110 °C exhibited the highest UV absorption capacity among all LNP samples. Many publications have reported that the presence of the conjunction structure formed by double bonds and/or carbonyl groups with a phenyl group may provide lignin with a strong UV absorption capacity.[43,44] However, the content of this conjunction structure in the extracted lignin was reduced with the enhancement of the pretreatment severity, which resulted in a decrease in the UV absorption capacity.[14,45] Combining the highest enzymatic efficiency at 110 °C (Fig. 3a), the LNPs obtained from 110 °C were selected to prepare the lignin-based sunscreen. Besides, an AFM image of the LNPs obtained under 110 °C (Fig. S6†) exhibited their nanoscale size, further demonstrating that the collected LNPs might be a desirable anti-ultraviolet additive for sunscreen production.

As exhibited in Fig. 7a, different amounts of LNPs were mixed with a commercial sunscreen with an SPF of 15. The addition of 4% LNPs resulted in a similar light-yellow color as that of the blank sample without LNP addition. The UV transmittances for produced sunscreens are shown in Fig. 7c, and their SPF values were further calculated as demonstrated in Fig. 7d according to a previously reported method.[6] The produced sunscreen displayed a decrease in UV transmittance within UVA (320–400 nm) and UVB (290–320 nm) ranges with an increasing content of LNPs, indicating an excellent UV blocking performance. The SPF of the lignin-based sunscreen adding 2% LNPs reached 34.15, exceeding that of commercial SPF 30 sunscreen with a measured SPF value of 32.06. With the addition of LNPs (4%), the SPF value of the obtained sunscreen reached up to 58.46, which was 1.82 times and 1.28 times higher than those of SPF 30 and SPF 50 sunscreens, respectively. The measured results indicated that the prepared sunscreen possessed excellent UV resistant properties. The produced sunscreen did not cause any contamination on the human skin as demonstrated in Fig. 7e. Thus, the GSL

Published on 02 February 2024. Downloaded on 5/23/2026 12:12:36 AM.

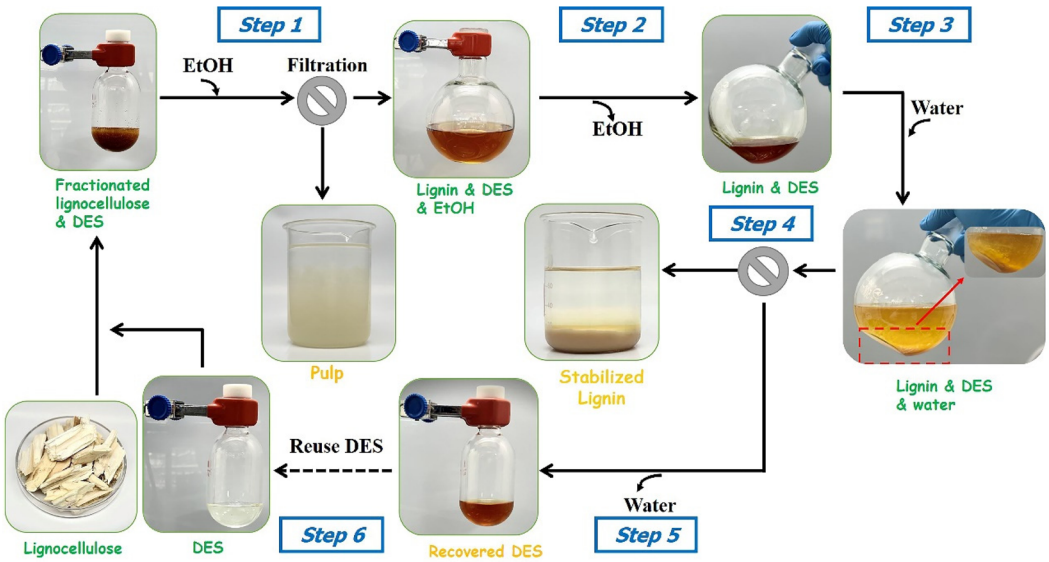

Fig. 8 The fractionation protocol of *Boehmeria nivea* stalks using the ChCl : GA DES and recovery of DES.

extracted from *Boehmeria nivea* stalks can be used as an anti-ultraviolet additive for lignin-based sunscreen preparation.

3.5 DES recovery

Fig. 8 shows an approach of lignocellulose fractionation using the ChCl : GA DES and DES recovery. After filtration, the anti-solvent (ethanol) was used to wash the cellulose residue. Pulp was obtained *via* further ultrasonic treatment for 10 s in step 1. Subsequently, the mixture containing ethanol, lignin, and DES was further concentrated by removing ethanol using rotary evaporation at 40 °C (step 2). The addition of deionized water in step 3 led to the precipitation of GSL. After filtration and washing with DI, the protected lignin with a purity of 95.60% was obtained in step 4. DES was recovered by removing deionized water in step 5 and reused for lignocellulose fractionation in step 6. In this system, the cellulose fraction and lignin fraction were effectively separated from *Boehmeria nivea* stalks. The ChCl : GA DES used in the biomass fractionation process was easily recycled with an ideal yield of 96.80%.

4. Conclusion

Herein, a new DES composed of ChCl and GA was developed for lignocellulose valorization. Under optimal pretreatment conditions (T130M1:4t30), the ChCl : GA DES exhibited higher removal of lignin (90.01%) and hemicellulose (85.17%) from *Boehmeria nivea* stalks than the ChCl : LA DES. MD simulations indicated that the ChCl : GA DES showed a higher total binding energy (ΔE) with lignin than the ChCl : LA DES, resulting in a higher dissolution of lignin. Furthermore, the ChCl : GA DES pretreatment caused cellulose functionalization by introducing aldehyde groups on the cellulose surface, which was not found in the pretreatment using the ChCl : LA DES. The cellulose residue can be used for antibacterial paper fabrication or industrial papermaking. Meanwhile, GA prevented lignin condensation by a stabilization approach. The stabilized lignin containing 69.39% β-O-4 linkages can be used for phenolic monomer production with a bio-oil yield of 59.60% and lignin-based sunscreen preparation with a SPF of 58.46. Moreover, the ChCl : GA DES was recycled with a desirable yield of 96.80%. Therefore, this study provided a functional DES for lignocellulose valorization *via* lignin stabilization and cellulose functionalization.

Author contributions

Zhen Zhang: date analysis and writing-original draft; Hairui Ji: conceptualization, investigation, and writing-review & editing; Pingli Lv: software and methodology; Xingxiang Ji: supervision and writing-review & editing; Zhongjian Tian: supervision and writing-review & editing; Jiachuan Chen: supervision and writing-review & editing.

Conflicts of interest

There are no conflicts to declare.

Acknowledgements

The authors would like to express gratitude for the support from the Program of National Natural Science Foundation of China (32271800), the Basic Research Integration Projects of Science, Education, and Industry of Qilu University of Technology (2022PY039), the Jinan Innovation Team (2021GXRC023), and the QUTJBZ Program (2022JBZ01-05).

 This journal is © The Royal Society of Chemistry 2024

Published on 02 February 2024. Downloaded on 5/23/2026 12:12:36 AM.

References

1 M. G. Morán-Aguilar, M. Calderón-Santoyo, R. P. S. Oliveira, M. G. Aguilar-Uscanga and J. M. Domínguez, *Carbohydr. Polym.*, 2022, **298**, 120097.
2 X.-J. Shen, J.-L. Wen, Q.-Q. Mei, X. Chen, D. Sun, T.-Q. Yuan and R.-C. Sun, *Green Chem.*, 2019, **21**, 275–283.
3 M. Wu, L. Gong, C. Ma and Y.-C. He, *Bioresour. Technol.*, 2021, **340**, 125695.
4 J. Cheng, C. Huang, Y. Zhan, S. Han, J. Wang, X. Meng, C. G. Yoo, G. Fang and A. J. Ragauskas, *Chem. Eng. J.*, 2022, **443**, 136395.
5 A. Ullah, Y. Zhang, C. Liu, Q. Qiao, Q. Shao and J. Shi, *Bioresour. Technol.*, 2023, **369**, 128394.
6 Y. Lyu, X.-X. Ji, Z. Tian, H. Ji, F. Zhang, L. Dai, H. Xie and C. Si, *Int. J. Biol. Macromol.*, 2023, **230**, 123122.
7 J. Yang, S. Wang, F. Bai, X. Lu, W. He, Z. Fang, N. Zhu and K. Guo, *Chem. Eng. J.*, 2023, **454**, 140480.
8 A. Mena-García, A. I. Ruiz-Matute, A. C. Soria and M. L. Sanz, *TrAC, Trends Anal. Chem.*, 2019, **119**, 115612.
9 J. Xu, P. Zhou, X. Liu, L. Yuan, C. Zhang and L. Dai, *ChemSusChem*, 2021, **14**, 2740–2748.
10 Y. Yu, D. Wang, L. Chen, H. Qi, A. Liu, M. Deng, X. Wu and K. Wang, *Ind. Crops Prod.*, 2022, **187**, 115542.
11 Y. Wang, X. Meng, K. Jeong, S. Li, G. Leem, K. H. Kim, Y. Pu, A. J. Ragauskas and C. G. Yoo, *ACS Sustainable Chem. Eng.*, 2020, **8**, 12542–12553.
12 Q. Ji, X. Yu, P. Wu, A. E.-G. A. Yagoub, L. Chen, A. T. Mustapha and C. Zhou, *Ind. Crops Prod.*, 2021, **173**, 114108.
13 H. Ji and P. Lv, *Green Chem.*, 2020, **22**, 1378–1387.
14 H. Ji, Y. Song, X. Zhang and T. Tan, *Bioresour. Technol.*, 2017, **238**, 575–581.
15 P. D. Muley, J. K. Mobley, X. Tong, B. Novak, J. Stevens, D. Moldovan, J. Shi and D. Boldor, *Energy Convers. Manage.*, 2019, **196**, 1080–1088.
16 L. Yao, P. Cui, X. Chen, C. G. Yoo, Q. Liu, X. Meng, L. Xiong, A. J. Ragauskas and H. Yang, *Bioresour. Technol.*, 2022, **350**, 126885.
17 Z. Chen, W. A. Jacoby and C. Wan, *Bioresour. Technol.*, 2019, **279**, 281–286.
18 W. Wang, F. Gu, J. Y. Zhu, K. Sun, Z. Cai, S. Yao, W. Wu and Y. Jin, *Ind. Crops Prod.*, 2020, **150**, 112423.
19 Z. Chen, X. Bai, L. A., H. Zhang and C. Wan, *ACS Sustainable Chem. Eng.*, 2020, **8**, 9783–9793.
20 Y. Liu, N. Deak, Z. Wang, H. Yu, L. Hameleers, E. Jurak, P. J. Deuss and K. Barta, *Nat. Commun.*, 2021, **12**, 5424.
21 S. Bertella, M. B. Figueirêdo, G. De Angelis, M. Mourez, C. Bourmaud, E. Amstad and J. S. Luterbacher, *ChemSusChem*, 2022, **15**, e202200270.
22 A. Sluiter, B. Hames, R. Ruiz, C. Scarlata and D. Crocker, *Determination of Structural Carbohydrates and Lignin in Biomass—NREL/TP-510-42618*, 2008.
23 P. D. Maibam and A. Goyal, *Bioresour. Technol.*, 2022, **351**, 127057.
24 H. J. C. Berendsen, D. van der Spoel and R. van Drunen, *Comput. Phys. Commun.*, 1995, **91**, 43–56.
25 B. Hess, C. Kutzner, D. van der Spoel and E. Lindahl, *J. Chem. Theory Comput.*, 2008, **4**, 435–447.
26 D. Van Der Spoel, E. Lindahl, B. Hess, G. Groenhof, A. E. Mark and H. J. C. Berendsen, *J. Comput. Chem.*, 2005, **26**, 1701–1718.
27 B. G. Janesko, *Phys. Chem. Chem. Phys.*, 2011, **13**, 11393–11401.
28 W. Ji, Z. Ding, J. Liu, Q. Song, X. Xia, H. Gao, H. Wang and W. Gu, *Energy Fuels*, 2012, **26**, 6393–6403.
29 Y. Zhu, J. Yan, C. Liu and D. Zhang, *Biopolymers*, 2017, **107**, e23022.
30 R. Liu, L. Dai, C. Xu, K. Wang, C. Zheng and C. Si, *ChemSusChem*, 2020, **13**, 4266–4283.
31 Z. Zhang, J. Xu, J. Xie, S. Zhu, B. Wang, J. Li and K. Chen, *Carbohydr. Polym.*, 2022, **290**, 119472.
32 Z. Ling, Z. Guo, C. Huang, L. Yao and F. Xu, *Bioresour. Technol.*, 2020, **305**, 123025.
33 A. Mnasri, H. Dhaouadi, R. Khiari, S. Halila and E. Mauret, *Carbohydr. Polym.*, 2022, **292**, 119606.
34 R. Zhai, J. Hu and J. N. Saddler, *Sustainable Energy Fuels*, 2018, **2**, 1048–1056.
35 J. A. Ávila Ramírez, C. J. Suriano, P. Cerrutti and M. L. Foresti, *Carbohydr. Polym.*, 2014, **114**, 416–423.
36 G. Zeng, L. Zhang, B. Qi, J. Luo and Y. Wan, *Bioresour. Technol.*, 2023, **380**, 129085.
37 M. T. Amiri, G. R. Dick, Y. M. Questell-Santiago and J. S. Luterbacher, *Nat. Protoc.*, 2019, **14**, 921–954.
38 H. Cao, R. Liu, B. Li, Y. Wu, K. Wang, Y. Yang, A. Li, Y. Zhuang, D. Cai and P. Qin, *Ind. Crops Prod.*, 2022, **177**, 114480.
39 W. Lan, M. T. Amiri, C. M. Hunston and J. S. Luterbacher, *Angew. Chem., Int. Ed.*, 2018, **57**, 1356–1360.
40 L. Shuai, M. T. Amiri, Y. M. Questell-Santiago, F. Héroguel, Y. Li, H. Kim, R. Meilan, C. Chapple, J. Ralph and J. S. Luterbacher, *Science*, 2016, **354**, 329–333.
41 S. Liu and H. Ji, *Cellulose*, 2023, **30**, 1503–1515.
42 X. Liu, Z. Jiang, S. Feng, H. Zhang, J. Li and C. Hu, *Fuel*, 2019, **244**, 247–257.
43 M. H. Tran, D.-P. Phan and E. Y. Lee, *Green Chem.*, 2021, **23**, 4633–4646.
44 Y. Qian, X. Qiu and S. Zhu, *Green Chem.*, 2015, **17**, 320–324.
45 H. Ji, L. Wang, Z. Pang, W. Zhu, G. Yang and C. Dong, *Cellulose*, 2020, **27**, 7561–7573.